

Preparation and properties of novel Cu-based bulk metallic glasses $\text{Cu}_{55-x}\text{Zr}_{37}\text{Ti}_8\text{In}_x$

Jin-hong PI^{1,2}, Ye PAN¹, Ji-li WU¹, Lu ZHANG¹, Xian-cong HE²

1. Jiangsu Key Laboratory for Advanced Metallic Materials, School of Materials Science and Engineering,
Southeast University, Nanjing 211189, China;

2. School of Materials Engineering, Nanjing Institute of Technology, Nanjing 211167, China

Received 12 September 2012; accepted 18 May 2013

Abstract: The glassy rods were successfully fabricated in the Cu–Zr–Ti–In alloy system by casting into a copper mold. The value of ΔT_x reaches a maximum of 66 K for the BMG $\text{Cu}_{50}\text{Zr}_{37}\text{Ti}_8\text{In}_5$ alloy. The reasons for enhancing glass forming ability of Cu-based BMGs with the addition of indium were discussed from atomic size and thermodynamics. Alternatively, the BMG $\text{Cu}_{52}\text{Zr}_{37}\text{Ti}_8\text{In}_3$ exhibits the highest compressive strength (1981 MPa) and the best plasticity among glassy $\text{Cu}_{55-x}\text{Zr}_{37}\text{Ti}_8\text{In}_x$ ($x \leq 5$). The total plastic deformation of $\text{Cu}_{52}\text{Zr}_{37}\text{Ti}_8\text{In}_3$ before fracture approaches 1.2%.

Key words: Cu–Zr–Ti–In alloy; indium; Cu-based alloy; bulk metallic glass; glass forming ability; mechanical properties

1 Introduction

Bulk metallic glasses (BMGs) have excellent properties such as high strength [1], large elastic elongation [2], excellent corrosion resistance [3], good soft magnetic properties [4], smooth surface and viscous deformability [5]. Now, lots of BMGs with different compositions have been developed in various systems such as Al-, Mg-, Zr-, Pd-, Ti-, Fe- and Cu-based alloys [6,7]. Compared with Zr- and Pd-based BMGs, Cu-based BMGs have attracted more and more attention, due to their relative high glass forming ability (GFA), excellent mechanical and chemical properties and low cost [8], and are also considered advanced engineering materials in future. Therefore, designing new compositions of Cu-based BMGs and improving the properties of Cu-based BMGs are worthy to be studied.

Up to date, Cu-based BMGs have been developed in systems, such as Cu–Zr–Ti [9], Cu–Zr–Al [10] and Cu–Zr–Ag [11]. Since the Cu-based BMGs in Cu–Zr–Ti system have relative high GFA [3] without noble metals, such as Pd and Ag, many researchers have shown interests in the investigation of this alloy system and in improving its GFA by minor alloying [12,13]. However, no Cu-based BMGs in Cu–Zr–Ti–In system were

reported according to the published references. According to Ref. [14], the atomic radii of Cu, Zr, Ti, and In are 0.127, 0.160, 0.145, and 0.162 nm, respectively. And the mixture heat of In–Cu, In–Zr and In–Ti are 10, -25 and -5 kJ/mol, respectively [15]. As we know, the GFA can be strongly affected by the large negative heat of mixing among the constituent elements [10]. Therefore, the atomic size range is expanded and the mixing heat may be reduced after the addition of element In, which may be favorable for improving GFA. Additionally, ZHENG et al [16] successfully enhanced the ductility of Ti-based BMG by adding soft atom, element In. Therefore, a new series of BMGs in Cu–Zr–Ti–In systems were fabricated and characterized using $\text{Cu}_{55}\text{Zr}_{37}\text{Ti}_8$, of which the critical size is 3 mm in diameter, as a starting material [17] in this work.

2 Experimental

Mixtures of pure elements (the purity is between 99% and 99.99%) with the nominal composition of $\text{Cu}_{55-x}\text{Zr}_{37}\text{Ti}_8\text{In}_x$ ($x \leq 5$) were arc-melted under a Ti-gettered argon atmosphere. In order to ensure chemical homogeneity of ingots, each ingot was melted at least four times. Subsequently, the arc-melted ingot was re-melted and cast into a rod-shaped cavity in a

copper mold with a diameter of 3–4 mm. The microstructures of cross-sections of the samples were characterized using X-ray diffraction with a Cu K_α radiation (XRD, D8 Discovery) and scanning electron microscopy (SEM, JEOL JSM-6360LV). The glass transition temperature, the onset temperature of crystallization and the melting temperature were measured by differential scanning calorimetry (DSC) (NETZSCHSTA 449F3) with a heating rate of 20 K/min. Room temperature compressive property of each sample ($d=3$ mm×6 mm) was tested on materials testing machine (Instron MTS569) at a strain rate of 3×10^{-4} s⁻¹.

3 Results and discussion

Figure 1 shows the X-ray diffraction patterns of the as-cast BMGs Cu_{55-x}Zr₃₇Ti₈In_x ($x\leq 5$). It can be seen that when x increases from 0 to 5, all XRD patterns, except 4 mm-diameter Cu₅₄Zr₃₇Ti₈In₁ alloy rod, exhibit only a broad diffraction peak without any detectable sharp peaks of crystalline phases, indicating the formation of amorphous structure. In the XRD pattern of 4 mm-diameter Cu₅₄Zr₃₇Ti₈In₁ alloy rod, some sharp diffraction peaks, which are identified as Cu₁₀Zr₇, superimpose on the broad diffraction peak, suggesting the presence of a little of crystalline phases. Therefore, it can be proposed that the GFA of BMGs Cu–Zr–Ti increases with the addition of In.

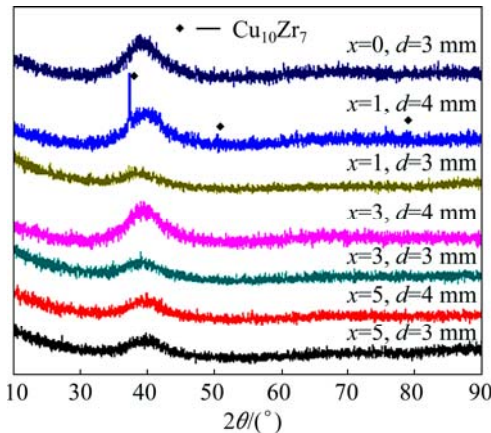


Fig. 1 XRD patterns of Cu_{55-x}Zr₃₇Ti₈In_x ($x\leq 5\%$) alloys

Figure 2 shows the DSC curves of the Cu_{55-x}Zr₃₇Ti₈In_x ($x\leq 5$) alloys ($d=3$ mm). The glass transition temperature (T_g), onset crystallization temperature (T_x), melting point of alloys (T_m) and liquidus temperature (T_l) are indicated by arrows in the DSC traces. The alloys exhibit distinct glass transitions, followed by super-cooled liquid regions, and then the exothermic reaction corresponding to crystallization. The values of T_g , T_x , ΔT_x ($\Delta T_x=T_x-T_g$), T_m , T_l , T_{rg} ($T_{rg}=T_g/T_l$) and γ ($\gamma=T_x/(T_g+T_l)$) are listed in Table 1.

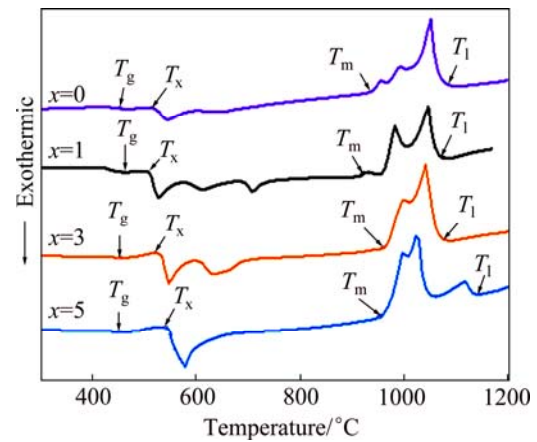


Fig. 2 DSC curves of Cu_{55-x}Zr₃₇Ti₈In_x ($x\leq 5$) BMGs at heating rate of 20 K/min

Table 1 Parameters of T_g , T_x , T_m , T_l , ΔT_x , γ and T_{rg} for BMGs Cu_{55-x}Zr₃₇Ti₈In_x ($x\leq 5$)

x	$T_g/^\circ\text{C}$	$T_x/^\circ\text{C}$	$T_m/^\circ\text{C}$	$T_l/^\circ\text{C}$	$\Delta T_x/^\circ\text{C}$	$T_{rg}=T_g/T_l$	γ
0	403	453	792	903	50	0.446	0.347
1	402	454	795	902	52	0.446	0.348
3	420	478	805	900	58	0.467	0.362
5	428	497	809	896	69	0.478	0.375

As we can see, both the T_g and T_x increase with increasing In content. The T_g increases from 402 °C at $x=1$ to 428 °C at $x=5$, while the T_x increases from 453 °C to 497 °C for In content, x , of 0–5. As a result, the super-cooled liquid region (ΔT_x) increases from 50 °C to 69 °C with increasing x from 0 to 5, indicating enhancement of GFA.

Additionally, a higher T_{rg} value indicates that competing crystalline phase can be restrained to form glassy phase at a relative low cooling rate, resulting in the high GFA [18]. It is reasonable to suppose that the addition of In element brings higher GFA because with In content increasing from 0 to 5%, T_{rg} increases from 0.446 to 0.478.

The results can be also explained by a thermodynamic approach. Previous works demonstrated that the smaller Gibbs free energy difference (ΔG_{l-s}) between the liquid and corresponding crystalline phases means the more restriction of competing crystalline phase and the better GFA. The value of ΔG_{l-s} can be estimated by the following equation:

$$\Delta G_{l-s} = \Delta H^{\text{mix}} - T\Delta S^{\text{mix}} \quad (1)$$

where ΔH^{mix} is the mixing enthalpy, ΔS^{mix} is the mixing entropy, and T is the temperature of the undercooled liquid. When predicting the GFA before experiments instead of evaluating the GFA after experiments, the

temperature of liquid alloy is actually unknown. Accordingly, the value of ΔG_{l-s} can not be calculated exactly with this expression. However, it is known that smaller ΔH^{mix} and larger ΔS result in smaller value of ΔG_{l-s} , which is favored to higher GFA. Therefore, considering the value of ΔS is positive, the liquid stability can be evaluated by the value of $\Delta H^{\text{mix}} \Delta S$ when the value of ΔH^{mix} is negative, that is, the more negative the value of $\Delta H^{\text{mix}} \Delta S$ is, the higher the GFA is expected.

The value of ΔH^{mix} can be calculated based on the regular melt model [19]:

$$\Delta H^{\text{mix}} = \sum_{i=1, i \neq j}^n \Omega_{ij} c_i c_j = 4 \sum_{i=1, i \neq j}^n \Delta H_{i-j}^{\text{mix}} c_i c_j \quad (2)$$

where Ω_{ij} is the interaction parameter between the i th and j th elements in regular solutions; $\Delta H_{i-j}^{\text{mix}}$ is the enthalpy of mixing of atomic pairs between the i th and j th elements; c_i and c_j are the atomic fraction of the i th and j th element respectively. The values of $\Delta H_{i-j}^{\text{mix}}$ of Cu–Zr, Cu–Ti, and Zr–Ti are –23, –9 and 0 kJ/mol, respectively [15].

ΔS can be determined by

$$\Delta S = -R \sum_{i=1}^n c_i \ln c_i \quad (3)$$

Accordingly, the values of calculated ΔH^{mix} , ΔS and $\Delta H^{\text{mix}} \Delta S$ of BMGs $\text{Cu}_{55-x}\text{Zr}_{37}\text{Ti}_8\text{In}_x$ ($x \leq 5\%$) are listed in Table 2. It can be easily seen that the value of $\Delta H^{\text{mix}} \Delta S$ increases with x increasing from 0 to 5, meaning an increase of GFA from the viewpoint of thermodynamics. Small amount of In addition ($x=1$) does not obviously improve the GFA of $\text{Cu}_{55}\text{Zr}_{37}\text{Ti}_8$, which means that simply increasing the amount of components in BMGs does not assure higher GFA. It can improve the GFA of BMGs only when the addition of alloying elements results in obviously smaller value of ΔG_{l-s} .

Table 2 Values of calculated ΔH^{mix} , ΔS and $\Delta H^{\text{mix}} \Delta S$ of BMGs $\text{Cu}_{55-x}\text{Zr}_{37}\text{Ti}_8\text{In}_x$ ($x \leq 5\%$)

x	$\Delta H^{\text{mix}}/(\text{kJ} \cdot \text{mol}^{-1})$	$\Delta S/(\text{J} \cdot \text{mol}^{-1} \cdot \text{K}^{-1})$	$\Delta H^{\text{mix}} \Delta S/(10^3 \text{J}^2 \cdot \text{mol}^{-2} \cdot \text{K}^{-1})$
0	–20.3	7.47	–151.7
1	–20.1	7.89	–158.6
3	–19.7	8.44	–166.5
5	–19.4	8.87	–171.9

What's more, with the addition of large atom In, the packing efficiency of atoms is improved, the complexity and mismatch of the alloy system are increased, and finally the GFA is improved.

Figure 3 shows the room temperature compressive curves of $\text{Cu}_{55-x}\text{Zr}_{37}\text{Ti}_8\text{In}_x$ ($x \leq 5\%$). The room temperature compressive strength of BMG $\text{Cu}_{52}\text{Zr}_{37}\text{Ti}_8\text{In}_3$ is high up

to 1981 MPa, which is the highest compressive strength among the tested BMGs in this work. It can also be seen that the total plastic deformation of $\text{Cu}_{52}\text{Zr}_{37}\text{Ti}_8\text{In}_3$ before fracture is about 1.2%. Further increase of In addition does not apparently help to strengthen the BMGs in our experimental conditions. It should be noted that compositions with different as-quenched structural configurations may show different degrees of densification, which can be reflected by the relative change of strength.

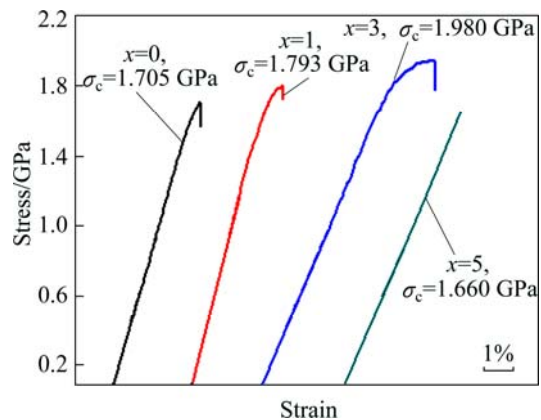


Fig. 3 Room temperature compressive curves of BMGs $\text{Cu}_{55-x}\text{Zr}_{37}\text{Ti}_8\text{In}_x$ ($x \leq 5\%$)

The fracture morphologies of $\text{Cu}_{55-x}\text{Zr}_{37}\text{Ti}_8\text{In}_x$ are shown in Fig. 4. The glassy $\text{Cu}_{50}\text{Zr}_{37}\text{Ti}_8\text{In}_5$ rod was crushed into pieces under compressive load.

From Fig. 4, typical vein patterns can be observed on the fracture surfaces. And when x increases from 0 to 3, the amount of shear bands on the specimen surfaces increases, and the vein patterns become more consecutive. As we know, the deformation of BMGs under compression is characterized by the formation of shear bands, their rapid propagation, and the sudden fracture of the sample. According to Ref. [8], a very high amount of shear is focused in the shear bands, since when the specimen fractures, a significant amount of energy is released, leading to a large temperature rise, and thus resulting in local softening or melting. The clearly resolidified droplets (pointed by arrows in Fig. 4) on the fracture prove that localized melting occurred. Clearly, more droplets can be found on the fracture of glassy $\text{Cu}_{54}\text{Zr}_{37}\text{Ti}_8\text{In}_1$ and $\text{Cu}_{52}\text{Zr}_{37}\text{Ti}_8\text{In}_3$. And the preferential breaking of local atomic clusters rather than inter-atomic bonds in crystalline solids leads to crack growth. Since the shear bands are large planar bands of “shear transformation zone” (STZ) [1], more shear bands means that more STZs are involved during deformation, and more homogenous deformation occurs accordingly. That's why glassy samples with more shear bands show better plasticity.

Many shear bands with an average spacing of around 5 μm can be clearly observed on the outer surface

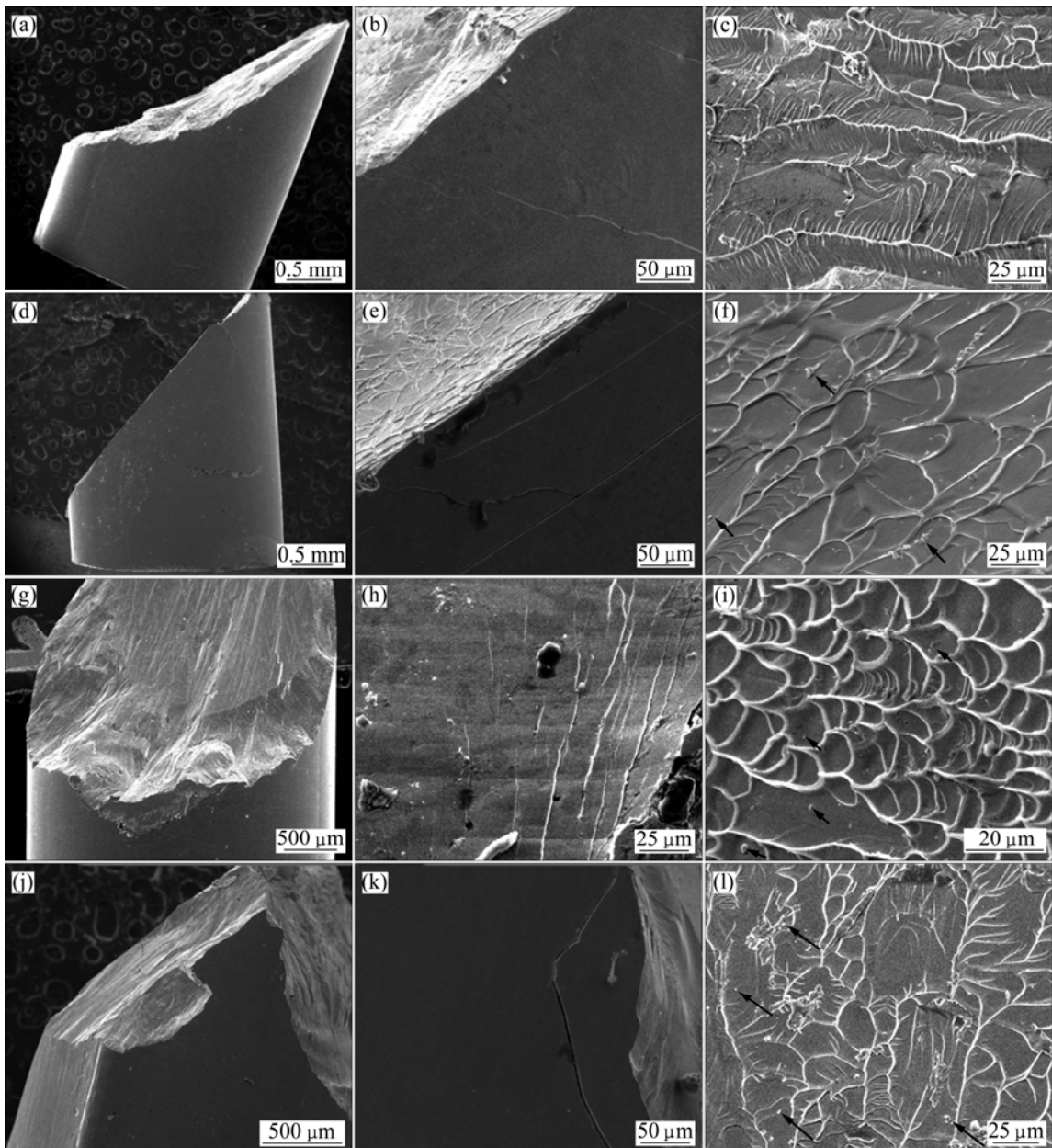


Fig. 4 Fracture morphologies of $\text{Cu}_{55-x}\text{Zr}_{37}\text{Ti}_8\text{In}_x$ ($x \leq 5$) glassy rods under compressive deformation mode: (a) $x=0$, side view of deformed specimen; (b) $x=0$, shear bands; (c) $x=0$, vein pattern; (d) $x=1$, side view of deformed specimen; (e) $x=1$, shear bands; (f) $x=1$, vein pattern; (g) $x=3$, side view of deformed specimen; (h) $x=3$, shear bands; (i) $x=3$, vein pattern; (j) $x=5$, side view of deformed specimen; (k) $x=5$, shear bands; (l) $x=5$, vein pattern

of $\text{Cu}_{52}\text{Zr}_{37}\text{Ti}_8\text{In}_3$. That's why glassy $\text{Cu}_{52}\text{Zr}_{37}\text{Ti}_8\text{In}_3$ exhibits clear plastic deformation during the fracture process, as shown in Fig. 4. Less shear bands can be observed on the outer surface of other samples, meaning less plasticity.

4 Conclusions

Fully amorphous structure was successfully fabricated by conventional arc-melting and copper mold suction-casting method in the novel alloy system $\text{Cu}_{55-x}\text{Zr}_{37}\text{Ti}_8\text{In}_x$ ($x \leq 5$) with diameter no less than 3–4

mm. The tested BMGs exhibit large temperature intervals of the super-cooled liquid region. The glass forming ability of Cu-based BMGs increases with the addition of In. The reasons are that the introduction of In element increases the complexity and mismatch of the alloy system and lowers the value of $\Delta H^{\text{mix}}\Delta S$, which results in lower Gibbs free energy difference between the liquid and the crystalline phases. Meanwhile, the glassy $\text{Cu}_{52}\text{Zr}_{37}\text{Ti}_8\text{In}_3$ exhibits the highest compressive strength (1981 MPa) among the tested BMGs, and the total elastic deformation of $\text{Cu}_{55-x}\text{Zr}_{37}\text{Ti}_8\text{In}_x$ ($x \leq 5$) before fracture increases with x .

References

[1] TREXLER M M, THADHANI N N. Mechanical properties of bulk metallic glasses [J]. *Prog Mater Sci*, 2010, 55: 759–839.

[2] SCHNEIDER S. Bulk metallic glasses [J]. *J Phys: Condens Matter*, 2001, 13: 7723–7736.

[3] KOU H C, LI Y, ZHANG T B, LI J, LI J S. Electrochemical corrosion properties of Zr- and Ti-based bulk metallic glasses [J]. *Transactions of Nonferrous Metals Society of China*, 2011, 21: 552–557.

[4] KOVALENKO N P, KRASNY Y P, KREY U. Physics of amorphous metals [M]. Weinheim: Wiley-VCH Verlag GmbH, 2001: 135–179.

[5] LI H, JIAO Z, GAO J, LU Z. Synthesis of bulk glassy Fe–C–Si–Ga alloys with high glass-forming ability and good soft-magnetic properties [J]. *Intermetallics*, 2010, 18: 1821–1825.

[6] KUZMIN O V, PEI Y T, HOSSON J T M D. Size effects and ductility of Al-based metallic glass [J]. *Scripta Materialia*, 2012, 67: 344–347.

[7] INOUE A, TAKEUCHI A. Recent development and application products of bulk glassy alloys [J]. *Acta Materialia*, 2011, 59(6): 2243–2267.

[8] SURYANARAYANA C, INOUE A. Bulk metallic glasses [M]. New York: CRC Press, 2011: 431–433.

[9] FU H, ZHANG H, WANG H, HU Z. Cu-based bulk amorphous alloy with larger glass-forming ability and supercooled liquid region [J]. *J Alloys Compd*, 2008, 458: 390–393.

[10] XU H W, DU Y L, DENG Y. Effects of Y addition on structural and mechanical properties of Cu–Zr–Ti–Sn bulk metallic glasses [J]. *Transactions of Nonferrous Metals Society of China*, 2012, 22: 842–846.

[11] WANG Q, QIANG J, WANG Y, XIA J, DONG C. Bulk metallic glass formation in Cu–Zr–Ti ternary system [J]. *J Non Cryst Solids*, 2007, 353: 3425–3428.

[12] MILLER M K, LIAW P K. Bulk metallic glasses [M]. New York: Springer, 2007: 13–16.

[13] KONG J, XIONG D S, YUAN Q X, YE Z T. Strengthening bulk metallic glasses with minor alloying additions [J]. *Transactions of Nonferrous Metals Society of China*, 2006, 16: s598–s602.

[14] XIA J H, QIANG J B, WANG Y M, WANG Q, DONG C. Cu–Zr–Ag bulk metallic glasses based on Cu₈Zr₅ icosahedron [J]. *Mater Sci Eng A*, 2007, 449: 281–284.

[15] GAL W F, TOTEMEIER T C. Smithells metals reference book [M]. Burlington: Elsevier Butterworth-Heinemann, 2004: 236–286.

[16] ZHENG N, QU R, PAULY S, CALIN M, GEMMING T, ZHANG Z. Design of ductile bulk metallic glasses by adding “soft” atoms [J]. *Appl Phys Lett*, 2012, 100(14): 141901.

[17] WU J L, PAN Y, PI J H, ZHANG L. Fabrication of Cu-rich bulk metallic glass composites via solidification method [C]//International Union of Materials Research Society—international Conference in Asia (IUMRS-ICA-2012). Switzerlan: TTP Ltd, 2012.

[18] GENG J Y, SUN Y F, WANG L G, ZHU S J, LIU L Z, GUAN S K. Effect of Al addition on formation and mechanical properties of Mg–Cu–Gd bulk metallic glass [J]. *Transactions of Nonferrous Metals Society of China*, 2007, 17: 907–912.

[19] ZHANG Q, ZHANG H, DENG Y, DING B, HU Z. Bulk metallic glass formation of Cu–Zr–Ti–Sn alloys [J]. *Scripta Mater*, 2003, 49: 273–278.

新型铜基块体非晶合金 Cu_{55-x}Zr₃₇Ti₈In_x 的制备及性能

皮锦红^{1,2}, 潘冶¹, 吴继礼¹, 张露¹, 贺显聪²

1. 东南大学 材料科学与工程学院, 江苏省先进金属材料重点实验室, 南京 211189;
2. 南京工程学院 材料工程学院, 南京 211167

摘要: 利用铜模吸铸法合成 Cu–Zr–Ti–In 非晶棒。块体非晶合金 Cu₅₀Zr₃₇Ti₈In₅ 的 ΔT_g 值最大, 为 66 K。从原子尺寸大小和热力学角度分析在铜基非晶合金中添加适量 In 元素后能够提高其非晶形成能力的原因。在所测的块体非晶合金 Cu_{55-x}Zr₃₇Ti₈In_x ($x \leq 5$) 中, Cu₅₂Zr₃₇Ti₈In₃ 表现出最高的抗压强度(1981 MPa)和最佳的塑性, 其在压缩断裂前的总塑性变形量约为 1.2%。

关键词: Cu–Zr–Ti–In 合金; 钢; Cu 基合金; 块体非晶合金; 非晶形成能力; 力学性能

(Edited by Hua YANG)